Synthesis of a Fully Conjugated Phthalocyanine-Diketopyrrolopyrrole-Phthalocyanine Triad as Low Band Gap Donor in Small Molecule Bulk Heterojunction Solar Cells

Desiré Molina,[a] Antonio Guerrero,[b] Germà Garcia-Belmonte,*[b] Fernando Fernández-Lázaro,[a] and Ángela Sastre-Santos*[a]

We describe the synthesis and photovoltaic properties of a fully conjugated phthalocyanine-diketopyrrolopyrrole-phthalocyanine triad (ZnPc-DPP-ZnPc) that presents strong visible absorption from 400 to 900 nm. The synthesis of the phthalocyanine with full conjugation to diketopyrrolopyrrole provides access to a new family of low band gap materials (<1.6 eV). Organic solar cells employing bulk heterojunction ZnPc-DPP-ZnPc:PC$_{70}$BM films using MoO$_3$ as anodic interfacial layer (IFL) show a power conversion efficiency of 1.04 %. The power conversion efficiency decreases considerably by using PEDOT:PSS as interfacial layer as a consequence of protonation of the ZnPc.

Introduction

Although most commercial photovoltaic devices are made from silicon, organic solar cells (OSCs) are a promising alternative that can potentially provide light-weight, low-cost and flexibility advantages.[1] While polymer-based donor materials are one of the most important components in organic bulk heterojunctions (BHJ), where they operate as donors in the active layer,[2] small molecule-based donor materials are an interesting alternative offering several promising advantages over their polymeric counterparts such as monodispersity and well-defined structure, easy purification, and better reproducibility (less batch-to-batch variation).[3] Recently, power conversion efficiencies (PCEs) obtained with single-molecule BHJ OSCs have been approaching those of conjugated polymers, and PCEs can exceed 7%.[4] However, this type of material presents other challenges such as the generation of high quality films in which interconnectivity between the domains is sufficient. In this context, the selection of a suitable interfacial layer (IFL) is key to obtain optimum efficiencies.

On the other hand, devices based on both polymer and small molecule absorbers are still unable to utilize a significant part of the red and infrared region of the solar spectrum, which ultimately limits their maximum achievable efficiency. Indeed, to date, examples in which contribution to the photocurrent takes place up to 900 nm (band gap <1.6 eV) with enough driving force to provide efficient charge separation are rare.[2b,5]

Phthalocyanines (Pcs) and diketopyrrolopyrroles (DPPs) are two of the most extensively investigated molecules in organic photovoltaics because of their outstanding chemical and physical properties. Pcs are porphyrin analogues with, generally, planar structure and high conjugation of the central ring (18 π electrons). They present interesting properties for application in photovoltaic cells, especially strong absorbance in the visible and near-infrared radiation region and high thermal and chemical stabilities.[6] Few examples have so far been reported in which soluble Pc derivatives have been blended with acceptor materials to form BHJ active layers.[7] Record efficiencies using Pcs up to 1.6% in solution-processed BHJs have been described by Torres and Bäuerle using RuPcs that were axially functionalized with pyridyl-dendritic oligothienylenes blended with methyl [6,6]-phenyl-C$_{71}$-butyrate (PC$_{70}$BM).[8]

On the other hand, DPPs possess exceptional absorbance properties in the 500–600 nm region, strong fluorescent performance, and high stability. A common feature of DPP-based materials is their relatively high oxidation potential, leading to high-energy charge separated states when combined with fullerenes, and correspondingly high voltages are obtained in solar cells. For these reasons DPPs, either as polymers or as single molecules, are being investigated as active layers for a range of OSC devices.[9] Nguyen and co-workers reported DPP-containing single-molecule donors that achieved up to 4.8% PCEs with PC$_{70}$BM in solution-processed BHJ devices.[10]

[a] División de Química Orgánica, Instituto de Bioingeniería,
    Universidad Miguel Hernández,
    Avda. de la Universidad, s/n, 03202 Elche, Spain
    E-mail: asastre@umh.es
    http://quimicaorganica.umh.es/
[b] Photovoltaic and Optoelectronic Devices Group, Departament
    de Física, Universitat Jaume I,
    12071 Castelló, Spain
    E-mail: garciag@fca.uji.es
    http://www.elp.uji.es/

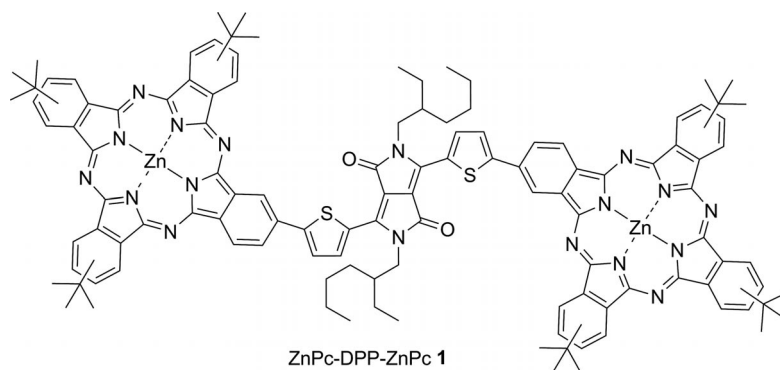G. Garcia-Belmonte, Á. Sastre-Santos et al.

Figure 1. Chemical structure of ZnPc-DPP-ZnPc **1**.

The combination of the exceptional absorption characteristics of both Pcs and DPPs could provide highly light-absorbing single molecule donor materials in a broad visible/near-infrared spectral region. Furthermore, molecules with two units of Pc covalently attached to the opposite positions of a DPP unit would allow the strong donor nature of the phthalocyanine to enhance the push-pull nature of the molecule in a centrosymmetric configuration, leading to increased intermolecular interaction and to a reduction in energetic disorder for charge transport.[11]

Here, we describe the synthesis of a strong light-harvester donor that presents wide visible absorption from 400 to 900 nm and is ready to be used in small-molecule BHJ OSCs: a fully conjugated molecule that combines two planar aromatic zinc phthalocyanine units with the rigid π-conjugated DPP core, ZnPc-DPP-ZnPc **1** (Figure 1). Moreover, we have also investigated the influence of the nature of the anodic IFL in the device performance by using either PEDOT:PSS or MoO_3 as IFL in solution-processed BHJ devices.

Results and Discussion

Synthesis

The synthesis of ZnPc-DPP-ZnPc **1** was carried out through two alternative pathways depicted in Scheme 1.

Route 1 involves Suzuki cross-coupling between DPP-bisboronic ester **3** and zinc tri-*tert*-butyl(iodo)phthalocyaninate [I(*t*Bu)$_3$ZnPc (**4**)] in 65% yield. DPP **3** was synthesized from 2,5-diethylhexyl-3,6-bis(thiophen-2′-yl)pyrrolo[3,4-*c*]-pyrrole-1,4-dione (T$_2$DPP, Figure 2), analogously as described in the literature.[12] In the second approach (Route 2), triad **1** was synthesized by statistical condensation of 4-*tert*-butylphthalonitrile and DPP-bis(phthalonitrile) **2** in the presence of zinc acetate in 9% yield. DPP-bis(phthalonitrile) **2** was synthesized in 81% yield from DPP-bis(boronic ester) **3** and 4-iodophthalonitrile through Suzuki reaction. Although the first pathway is a more convergent approach, giving rise to a higher global yield (24%
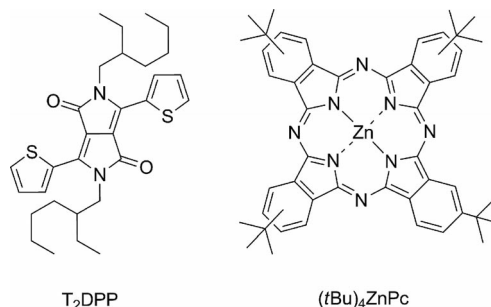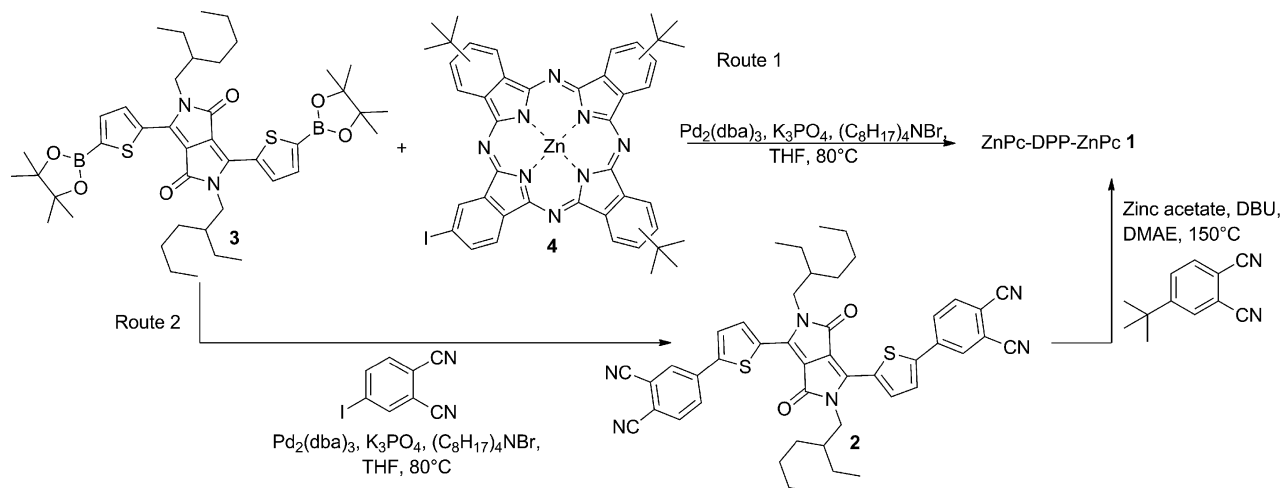

Figure 2. T$_2$DPP and (*t*Bu)$_4$ZnPc.

Scheme 1. Synthesis of ZnPc-DPP-ZnPc **1**.

taking into consideration the 30% yield in the synthesis of ZnPc 4[13]) of ZnPc-DPP-ZnPc 1, the second route (7% global yield) makes it possible to undertake statistical condensation of DPP-bis(phthalonitrile) 2 with different substituted phthalonitriles, thus paving the way to an unlimited variety of peripherally substituted phthalocyanines with different optoelectronic properties.

Characterization

As expected, ZnPc-DPP-ZnPc 1 is soluble in common organic solvents such as CHCl$_3$, tetrahydrofuran (THF), toluene, and chlorobenzene. Broad signals were obtained for 1 in the ^{1}H NMR spectra, even by using a coordinating solvent such as [D$_8$]THF, due to π–π stacking and also because of the mixture of regioisomers (see the Supporting Information).

The UV/Vis spectra of triad 1, (tBu)$_4$ZnPc, and T$_2$DPP in CHCl$_3$ as solvent are displayed in Figure 3a, and their data are included in Table 1. The existence of orbital overlap between the units in 1 leads to a strong interaction in the ground state, as reflected by the dramatic broadening and shift of the Q-band, which reaches the near-IR. The UV/Vis absorption spectrum of 1 was also studied in different solvents (THF and CHCl$_3$) and in the solid state (Figure 3b), which revealed significant differences. The spectrum recorded in THF shows a fine structure with maxima at 350 nm (Soret band), 674 and 729 nm (Q$_1$ and Q$_2$ bands, attributed to the existence of regioisomers), and a shoulder at 605 nm (from the DPP unit). This well-resolved spectrum is a consequence of the coordination of the solvent (THF) to the Zn ions, thus preventing aggregation in the diluted solution. A more coarse and broad UV/Vis spectrum with lower molar extinction coefficients was obtained in chloroform due to π–π aggregation effects, resulting in a high absorption from 500 to 900 nm. The Soret band moves only 2 nm to the red (to 352 nm), the shoulder appears at 617 nm, the Q$_1$ band undergoes a small bathochromic shift (from 674 nm in THF to 683 nm), the Q$_2$ band shifts 2 nm to the blue (727 nm), and one additional band appears at 768 nm. The broadest spectrum was obtained in the solid state; the Q band exhibited an amplitude of about 400 nm, covering part of the near-infrared to 1000 nm. (tBu)$_4$ZnPc revealed a fluorescence band located at 689 nm in CHCl$_3$ solution (Figure S7a). T$_2$DPP also showed a very high fluorescence in CHCl$_3$ solution at 564 and 609 nm (Figure S6b). However, fluorescence was totally quenched in 1,
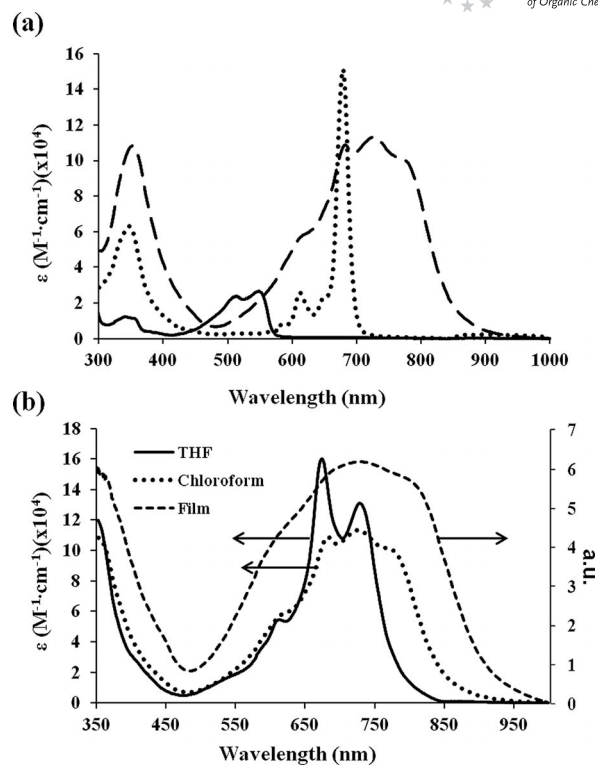

Figure 3. UV/Vis spectra in CHCl$_3$ as solvent of (a) ZnPc-DPP-ZnPc 1 (dashed line), T$_2$DPP (full line), and (tBu)$_4$ZnPc (dotted line); (b) UV/Vis spectra of ZnPc-DPP-ZnPc 1 in CHCl$_3$ (dotted line), THF (full line), and in the solid state (dashed line).

which could be attributed to intramolecular energy and/or electron transfer processes from the ZnPc to the DPP moiety (Table 1).

Cyclic voltammetric studies performed on a THF solution of ZnPc-DPP-ZnPc 1 containing 0.1 M Bu$_4$NPF$_6$ as supporting electrolyte, showed three oxidation peaks at 0.1, 0.3, and 0.5 V and two reduction peaks at –1.5 and –1.7 V vs. Fc/Fc$^+$. The oxidation peaks were cathodically shifted compared with the first oxidation of (tBu)$_4$ZnPc (0.5 V) and the first and second oxidation peaks of the T$_2$DPP reference compound (0.6 and 1.1 V), revealing a strong coupling among all the moieties in the ground state. This coupling was also observed by comparing the more negative shift of the reduction peaks of the triad with the first reduction potential of the (tBu)$_4$ZnPc (–1.2 V), and the first reduction potential of the T$_2$DPP (–1.6 V) (Figure 4 and Table 1).

Table 1. Optical and electrochemical parameters.

Dye	Absorbance λ_{max} [nm][a]	Emission λ_{max} [nm][a]	E_{ox1} [V][b]	E_{ox2} [V][b]	E_{ox3} [V][b]	E_{red1} [V][b]	E_{red2} [V][b]	E_g^{opt} [eV][c]	E_g^{CV} [eV][d]	HOMO [eV][e]	LUMO [eV][f]
T$_2$DPP	548	564[g]	0.6	1.1	–	–1.6	–	2.23	2.22	–5.34	–3.12
ZnPc-DPP-ZnPc 1	694	–	0.1	0.3	0.5	–1.5	–1.7	–	1.60	–4.90	–3.33
(tBu)$_4$ZnPc	679	689[h]	0.5	–	–	–1.2	–	1.82	1.70	–5.42	–3.60

[a] Absorption and emission spectra were measured in chloroform. [b] Redox potentials were measured in THF with 0.1 M Bu$_4$NPF$_6$ vs. Fc/Fc$^+$, with Pt counter electrode. [c] E_g^{opt} was determined from the intersection of normalized absorption and emission spectra registered in chloroform. [d] E_g^{CV} was calculated by $E_g^{CV} = E_{red1} - E_{ox1}$. [e] HOMO was calculated by HOMO $= -E_{ox1}$ (vs. Fc/Fc$^+$) $- 4.8$. [f] LUMO was calculated by LUMO $=$ HOMO $+ E_g$ (CV or opt). [g] Excitation wavelength (λ_{exc}) was 530 nm. [h] $\lambda_{exc} = 630$ nm.

G. Garcia-Belmonte, Á. Sastre-Santos et al.
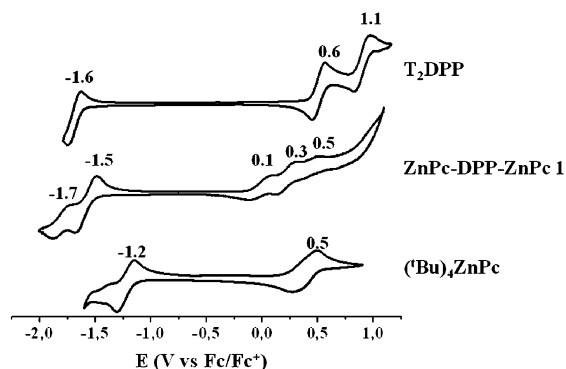

Figure 4. Cyclic voltammograms (100 mV s^{-1}) vs. Fc/Fc$^+$ of 0.5 mM ZnPc-DPP-ZnPc **1** (middle), and reference compounds, (*t*Bu)$_4$ZnPc (bottom) and T$_2$DPP (top) in THF containing 0.10 M Bu$_4$NPF$_6$ as supporting electrolyte.

The energies of the HOMO and LUMO of ZnPc-DPP-ZnPc **1** were determined to be approximately –4.90 and –3.33 eV, respectively, calculated from the electrochemical oxidation and reduction potentials. The HOMO and LUMO energy values suggest that the frontier molecular orbitals line up favorably with those of common fullerene acceptors such as PC$_{70}$BM that shows HOMO and LUMO levels of –6.0 and –4.0 eV, respectively, to generate useful V_{oc} in BHJ solar cells (Table 1).

Solar Cell Performance

Photovoltaic devices were fabricated by using the general architecture ITO/IFL/ZnPc-DPP-ZnPc **1**:PC$_{70}$BM/Ca/Ag. Poly(3,4-ethylenedioxythiophene):poly(styrenesulfonic acid) (PEDOT:PSS) was used as interfacial layer (IFL) anode. This IFL is known to be selective to holes and to reduce the roughness of the indium tin oxide (ITO), decreasing the risk of pinholes. The energy mismatch with the ITO and the HOMO level of the donor is sufficiently low to make an Ohmic contact (Figure 5). The solubility of **1** in halogenated solvents was adequate, and homogeneous films were obtained. Thus, a series of studies were conducted to optimize the power conversion efficiencies (PCE) using this material.
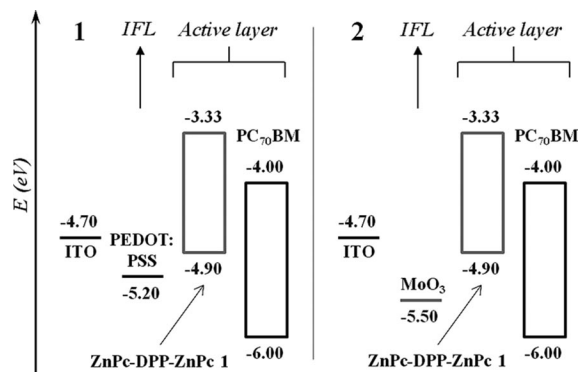

Figure 5. Energy level diagrams for the materials studied in this work: (1) IFL is PEDOT:PSS and (2) IFL is MoO$_3$.

The influence of the ratio of ZnPc-DPP-ZnPc **1**/PC$_{70}$BM was examined by looking at different compositions in chloroform. Details of the device fabrication process are described in the Experimental Section. We found that the use of a 1.5:1 ratio provided maximum efficiencies of 0.47% using PEDOT:PSS as IFL. For this combination, a photocurrent (J_{sc}) of 6 mA/cm^2 was obtained, indicating that charge separation with the acceptor material occurs readily. Open circuit voltage (V_{oc}) and fill factor (*FF*) were low, which seriously limited the device performance. Considering that other families of small molecule donors are very sensitive to the selection of the anode IFL, we also examined the use of MoO$_3$ as IFL.[14] For this system, efficiencies could be doubled to 1.04%, with relatively high V_{oc} for such a low band gap material and a short circuit current (J_{sc}) of 5.0 mA/cm^2. However, the *FF* remained low (38%). Typical current-voltage characteristics and external quantum efficiency (EQE) plots are shown in Figure 6, and the resulting photovoltaic parameters are summarized in Table 2. The EQE plot clearly shows that the contribution to the photocurrent extends up to 900 nm. Similar studies were performed by using active component (*t*Bu)$_4$ZnPc as donor. However, in our hands, due to the low homogeneity of the film, the photovoltaic parameters obtained were very poor.

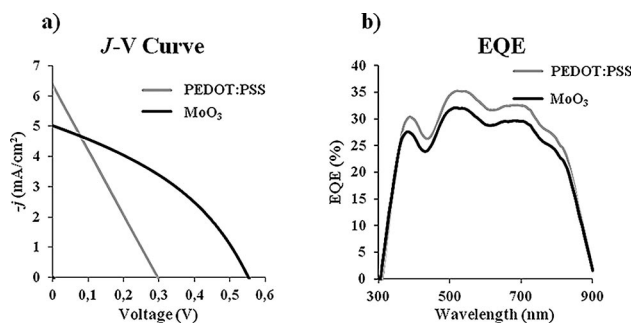Figure 6. (a) Current voltage characteristics of solar cells with an active layer comprised of ZnPc-DPP-ZnPc **1** and PC$_{70}$BM; (b) corresponding external quantum efficiency plots (black-line IFL is MoO$_3$, and grey-line IFL is PEDOT:PSS).

Table 2. Photovoltaic parameters.[a]

Entry	Anode IFL	J_{sc} [mA/cm^2]	V_{oc} [mV]	*FF* [%]	PCE [%]
1	PEDOT:PSS	6.36	296	25	0.47
2	MoO$_3$	5.00	551	38	1.04

[a] Devices fabricated in the configuration glass/ITO/IFL/ **1**:PC$_{70}$BM (ratio 1.5:1)/Ca/Ag.

Morphology measurements of ZnPc-DPP-ZnPc:PC$_{70}$BM using chloroform as solvent were evaluated by using atomic force microscopy (AFM; see Figure S8). The film was found to be smooth, with RMS roughness of 1.7 nm^2. Two different domains were visible, dark spots in a light matrix. It is possible that domains are not clearly interconnected, indicating that the morphology was not optimum. However, AFM does provide information at the surface level and better interconnectivity could be possible in the bulk of the active layer. At this stage, it appears that further material structural and device processing optimiza-

tions are needed. Nevertheless, these initial results are highly encouraging.

To better understand the differences between the results obtained by using PEDOT:PSS and MoO_3, we studied the potential interface degradation of the active layer using PEDOT:PSS. It has previously been reported that PEDOT:PSS used as IFL can protonate basic nitrogen atoms of the active layer materials, which hinders the transfer of holes from the active layer to the anode.[4c] This may be a source of increased series resistance and decreased *FF*. Additionally, a modification of the workfuntion at the interface can also explain the decreased V_{oc} observed. To test this possibility for ZnPc-DPP-ZnPc **1**, we measured the absorbance profile as a function of the concentration of trifluoroacetic acid; the resulting absorption profiles (Figure 7) showed significant changes immediately upon acid addition, namely, new low energy transitions, confirming that the chromophore backbone is influenced by protonation. This effect saturates when the trifluoroacetic acid (TFA) concentration is ten times greater than that of ZnPc-DPP-ZnPc **1**. Therefore, the use of PEDOT:PSS is not recommended for future device optimization for materials with similar combinations of structural moieties.
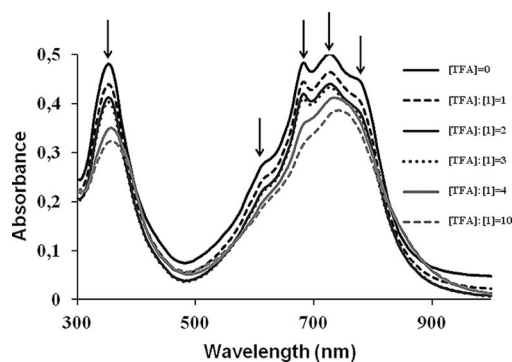

Figure 7. Absorbance of ZnPc-DPP-ZnPc **1** with different concentrations of trifluoroacetic acid (TFA) in chloroform. [**1**] = [ZnPc-DPP-ZnPc] = 4×10^{-6} M.

Conclusions

We have synthesized in a convergent manner and reported a full characterization of ZnPc-DPP-ZnPc **1**, which represents the first example of a family of materials containing conjugated phthalocyanine and diketopyrrolopyrrole subunits. This triad displays strong absorption from 500 to 900 nm, a low band gap, and a suitable alignment of the HOMO and LUMO levels, thus holding the promise of producing high efficiency OSCs. However, photovoltaic devices fabricated using the general architecture ITO/PEDOT:PSS/ZnPc-DPP-ZnPc **1**:$PC_{70}BM$/Ca/Ag showed efficiencies of 0.47%. Because we reasoned that these low values resulted from the acidic nature of PEDOT:PSS, devices were built using MoO_3 instead. This strategy proved to be effective, yielding an increase of 123% in the efficiency of the display devices. With this result, we have shown that

the interaction with the anode IFL is critical and needs to be taken into account in further development.

Our future research will focus on finding different peripherally substituted phthalocyanines with a lower HOMO level to gain higher V_{oc}, and to develop optimum device architectures that take advantage of the benefits offered by this type of D-A single molecule.

Experimental Section

Material and Methods: Solvents and reagents were obtained from commercial sources and were used as received. Column chromatography was performed with SiO_2 (40–63 μm), and TLC plates coated with SiO_2 $60F_{254}$ were visualized by UV light. NMR spectra were recorded at 25 °C with a Bruker AC300 spectrometer. The solvents for spectroscopic studies were of spectroscopic grade and were used as received. UV/Vis spectra were measured with a Helios Gamma spectrophotometer. IR spectra were measured with a Nicolet Impact 400D spectrophotometer. High-resolution mass spectra were obtained with a Bruker Microflex LRF20 matrix-assisted laser desorption/ionization time of flight (MALDI-TOF) spectrometer using dithranol as matrix. Melting points were measured with a Melting Point Apparatus SMP3. According to the IUPAC rules, "keto" is not a proper prefix; instead, "oxo" must be used in order to avoid that the C atom is counted twice (in "keto" and in "pyrrol"); however, the term "diketopyrrolopyrrole" instead of "dioxopyrrolopyrrole" is much more widespread, and therefore we have used the former in the text to make literature searches easier.

Device Fabrication and Characterization

OPV Device Fabrication: Patterned ITO-coated glass substrates with a resistivity of 10 Ω/cm² and thickness of about 200 nm were cleaned by sequential sonication at 50 °C in soap/deionized (DI) water, DI water, methanol, 2-propanol, and acetone for 30 min. ITO substrates were then treated for 30 min in a UV/O_3 oven (Jelight Co.). Next, either PEDOT:PSS or MoO_3 was deposited. PEDOT:PSS (Clevios P VP Al 4083) was spun-cast at 5000 rpm for 30 s and subsequently annealed at 150 °C in air for 15 min. Samples were then transferred to an N_2-filled glove box, and an additional drying step was carried out at 100 °C for 10 min to remove traces of water. MoO_3 (Sigma–Aldrich, 99.995%) was thermally deposited at a pressure of 1.0×10^{-6} Torr at a rate of 0.1 Å/s. Prior to active layer deposition, the MoO_3 films were transferred to air for ca. 2 min. Active layer solutions containing donor materials and $PC_{70}BM$ were formulated inside the glove box with optimum ratios (w/w): ZnPc-DPP-ZnPc **1**/$PC_{70}BM$ (1.5:1.0 in chloroform; 7 mg/mL). Active layer solutions were stirred at 45 °C for ca. 1 h. The active layer solution was spun-cast at 2000 rpm for 1 min after passing the solution through a 0.22 μm PTFE filter to afford active layers of 80 nm. To finish device fabrication, Ca (5 nm) and Ag (100 nm) were thermally evaporated, sequentially, at a base pressure of ca. 1.0×10^{-6} Torr. The top Ca/Ag electrodes were then encapsulated with UV-curable epoxy resin and a glass slide before testing. Each substrate had four cells with a defined average area of 0.25 cm².

Device Characterization: Current density-voltage measurements were carried out by illumination with a 1.5 G illumination source (1000 W m^{-2}) using an Abet Sun 2000 Solar Simulator. The light intensity was adjusted with a calibrated Si solar cell. UV/Vis data were obtained on films with a Cary 300 Bio Spectrophotometer. External Quantum Efficiency (EQE) measurements were performed by using a 150 W Xe lamp coupled with a monochromator

controlled by a computer. The light intensity was measured with an optical power meter 70310 from Oriel Instruments; an Si photodiode was used to calibrate the system.

Synthesis of ZnPc-DPP-ZnPc 1. Route 1: To a mixture of 2,5-bis-(2-ethylhexyl)-3,6-bis[5-(4,4,5,5-tetramethyl-1,3,2-dioxoborolan-2-yl)-thiophen-2-yl]-2,5-dihydropyrrolo[3,4-c]pyrrole-1,4-dione (16 mg, 0.02 mmol), zinc 6,16,23-tri-*tert*-butyl-2-iodophthalocyaninate (50 mg, 0.06 mmol), $Pd_2(dba)_3$ (0.6 mg, 0.0007 mmol) and tetra-octylammonium bromide (0.4 mg, 0.0013 mmol) dissolved in THF (1 mL), was added an aqueous 0.1 M solution of K_3PO_4 (0.0003 mg, 0.07 mmol) under argon, and the solution was heated to 80 °C overnight. The crude product was purified by silica gel chromatography (chloroform/THF, 200:1) to obtain a turquoise solid (26 mg, 65%). **Route 2:** A mixture of 4-*tert*-butylphthalonitrile (107 mg, 0.58 mmol), bis(phthalonitrile) derivative **2** (25 mg, 0.032 mmol) and zinc acetate (23 mg, 0.128 mmol) was heated to reflux in 2-(dimethylamino)ethanol (DMAE; 2.5 mL) under argon for 12 h. The crude product was precipitated and washed with methanol. The black solid obtained was purified by silica gel chromatography (chloroform/THF, 200:1) to obtain a turquoise solid (6 mg, 9%). M.p. >300 °C. ^{1}H NMR (300 MHz, [D$_8$]THF): δ = 9.96–7.74 (m, 28 H), 4.43 (s, 4 H) ppm. UV/Vis (CH$_2$Cl$_2$): λ_{max} (log ε) = 346 (5.05), 620 (4.85), 692 (5.04), 763 (5.02) nm. HRMS (MALDI-TOF): calcd. for $C_{118}H_{116}N_{18}O_2S_2Zn_2$ [M]$^+$ 2008.755; found 2088.782. FTIR (KBr): $\tilde{\nu}$ = 2953, 2921, 2856, 2195, 1664 (C=O lactam), 1608, 1548, 1486, 1444, 1393 (C–N), 1322, 1279, 1255 cm^{-1}. $C_{118}H_{116}N_{18}O_2S_2Zn_2\cdot2MeOH$ (2072.277): calcd. C 69.38, H 6.02, N 12.14, S 3.09; found C 69.03, H 5.86, N 11.84, S 3.42.

Synthesis of 2,5-Bis(2-ethylhexyl)-3,6-bis[5-(1,2-dicyano-4-phenyl)-thiophen-2-yl]-2,5-dihydropyrrolo[3,4-c]pyrrole-1,4-dione (2): An aqueous 0.1 M solution of K_3PO_4 (61 mg, 0.3 mmol) was added to a solution of 2,5-bis(2-ethylhexyl)-3,6-bis[5-(4,4,5,5-tetramethyl-1,3,2-dioxoborolan-2-yl)thiophen-2-yl]-2,5-dihydropyrrolo-[3,4-c]pyrrole-1,4-dione (92 mg, 0.09 mmol), $Pd_2(dba)_3$ (3 mg, 0.003 mmol), tetraoctylammonium bromide (3 mg, 0.005 mmol) and 4-iodophthalonitrile (70 mg, 0.36 mmol) in THF (5 mL) under argon, and the mixture was heated to 80 °C overnight. The crude product was purified by silica gel chromatography (chloroform/THF, 190:1) to obtain a metallic grey solid (58 mg, 81%). M.p. 287 °C. ^{1}H NMR (300 MHz, CDCl$_3$): δ = 8.93 (d, J = 4.2 Hz, 2 H), 8.05 (d, J = 1.8 Hz, 2 H), 7.97 (dd, J_1 = 8.3, J_2 = 1.8 Hz, 2 H), 7.85 (d, J = 8.3 Hz, 2 H), 7.63 (d, J = 4.2 Hz, 2 H), 4.06 (dd, J_1 = 7.9, J_2 = 2.4 Hz, 4 H), 1.88 (s, 2 H), 1.44–1.22 (m, 16 H), 0.94–0.85 (m, 12 H) ppm. UV/Vis (CH$_2$Cl$_2$): λ_{max} (log ε) = 368 (4.50), 579 (4.59), 621 (4.59) nm. HRMS (MALDI-TOF): calcd. for $C_{46}H_{44}N_6O_2S_2$ [M]$^+$ 776.298; found 776.293. FTIR (KBr): $\tilde{\nu}$ = 3093 (C–H), 2952 (CH$_3$), 2919 (CH$_2$), 2849 (CH$_2$), 2227 (C≡N), 1735, 1649 (C=O lactam), 1590, 1488, 1454, 1408, 1391 (C–N lactam), 1235 cm^{-1}.

Supporting Information (see footnote on the first page of this article): NMR, UV/Vis, MS and IR data of the new compounds; fluorescence spectra of reference compounds and AFM of the active layer.

Acknowledgments

[1] For reviews, see: a) G. Dennler, M. C. Scharber, C. J. Brabec, *Adv. Mater.* **2009**, *21*, 1323–1338; b) P. M. Beaujuge, J. M. J. Fréchet, *J. Am. Chem. Soc.* **2011**, *133*, 20009–20029; c) G. Li, R. R. Zhu, Y. Yang, *Nat. Photonics* **2012**, *6*, 153–161; d) S. Günes, H. Neugebauer, N. S. Sariciftci, *Chem. Rev.* **2007**, *107*, 1324–1338; e) A. Facchetti, *Chem. Mater.* **2011**, *23*, 733–758; f) B. Walker, C. Kim, T.-Q. Nguyen, *Chem. Mater.* **2011**, *23*, 470–482; g) J. Roncali, *Acc. Chem. Res.* **2009**, *42*, 1719–1730.

[2] a) G. Yu, J. Gao, J. C. Hummelen, F. Wudl, A. J. Heeger, *Science* **1995**, *270*, 1789–1791; b) L. Dou, J. You, J. Yang, C.-C. Chen, Y. He, S. Murase, T. Moriarty, K. Emery, G. Li, Y. Yang, *Nat. Photonics* **2012**, *6*, 180–185; c) C. E. Small, S. Chen, J. Subbiah, C. M. Amb, S. W. Tsang, T. H. Lai, J. R. Reynolds, F. So, *Nat. Photonics* **2012**, *6*, 115–120; d) H.-Y. Chen, J. Hou, S. Zhang, Y. Liang, G. Yang, Y. Yang, L. Yu, Y. Wu, G. Li, *Nat. Photonics* **2009**, *3*, 649–653; e) Y. J. Cheng, S. H. Yang, C. S. Hsu, *Chem. Rev.* **2009**, *109*, 5868–6923.

[3] a) M. T. Lloyd, J. E. Anthony, G. G. Malliaras, *Mater. Today* **2007**, *11*, 34–41; b) B. P. Rand, J. Genoe, P. Heremans, J. Poortmans, *Prog. Photovolt. Res. Appl.* **2007**, *15*, 659–676.

[4] a) A. Mishra, P. Bäuerle, *Angew. Chem. Int. Ed.* **2012**, *51*, 2020–2067; *Angew. Chem.* **2012**, *124*, 2060; b) Y. Sun, G. C. Welch, W. L. Leong, C. J. Takacs, G. C. Bazan, A. J. Heeger, *Nat. Mater.* **2012**, *11*, 44–48; c) T. S. van der Poll, J. A. Love, T.-C. Nguyen, G. C. Bazan, *Adv. Mater.* **2012**, *24*, 3646–3649; d) X. Liu, Y. Sun, L. A. Perez, W. Wen, M. F. Toney, A. J. Heeger, G. J. Bazan, *J. Am. Chem. Soc.* **2012**, *134*, 20609–20612; e) J. Zhou, X. Wan, Y. Liu, Y. Zuo, Z. Li, G. He, G. Long, W. Ni, C. Li, X. Su, Y. J. Chen, *J. Am. Chem. Soc.* **2012**, *134*, 16345–16351; f) A. Ko, K. Kyaw, D. H. Wang, V. Gupta, J. Zhang, S. Chand, G. C. Bazan, A. J. Heeger, *Adv. Mater.* **2013**, *25*, 2397–2402.

[5] J. You, L. Dou, K. Yoshimura, T. Kato, K. Ohya, T. Moriarty, K. Emery, C.-C. Chen, J. Gao, G. Li, Y. Yang, *Nat. Commun.* **2013**, *4*, 1446.

[6] a) G. de la Torre, C. G. Claessens, T. Torres, *Chem. Commun.* **2007**, 2000–2015; b) E. M. Barea, J. Ortiz, F. J. Payá, F. Fernández-Lázaro, F. Fabregat-Santiago, A. Sastre-Santos, J. Bisquert, *Energy Environ. Sci.* **2010**, *3*, 1985–1994.

[7] a) Q. Wang, Y. Li, X. Yan, M. Rathi, M. Ropp, D. Galipeau, J. Jiang, *Appl. Phys. Lett.* **2008**, *93*, 073303; b) A. Varotto, C.-Y. Nam, I. Radivojevic, J. P. C. Tomé, J. A. S. Cavaleiro, C. T. Black, C. M. Drain, *J. Am. Chem. Soc.* **2010**, *132*, 2552–2554; c) A. Sánchez-Díaz, R. Pacios, U. Muñecas, T. Torres, E. Palomares, *Org. Electron.* **2011**, *12*, 329–335; d) O. O. Adegoke, M. Ince, A. Mishra, A. Green, O. Varnavski, M. V. Martínez-Díaz, P. Bäuerle, T. Torres, T. Goodson, *J. Phys. Chem. C* **2013**, *117*, 20912–20918.

[8] M. K. R. Fischer, I. Lopez-Duarte, M. M. Wienk, M. V. Martinez-Diaz, R. A. J. Janssen, P. Bäuerle, T. Torres, *J. Am. Chem. Soc.* **2009**, *131*, 8669–8676.

[9] a) S. Qu, H. Tian, *Chem. Commun.* **2012**, *48*, 3039–3051; b) D. Chandran, K.-S. Lee, *Macromol. Res.* **2013**, *21*, 272–283; c) P. P. Boix, M. M. Wienk, R. A. J. Janssen, G. Garcia-Belmonte, *J. Phys. Chem. C* **2011**, *115*, 15075–15080.

[10] B. Walker, A. B. Tamayo, X. Dang, P. Zalar, J. H. Seo, A. García, M. Tantiwiwat, T. Nguyen, *Adv. Funct. Mater.* **2009**, *19*, 3063–3069.

[11] a) R. Fitzner, E. Reinold, A. Mishra, E. Mena-Osteritz, H. Ziehlke, C. Körner, K. Leo, M. Riede, M. Weil, O. Tsaryova, A. Weiß, C. Uhrich, M. Pfeiffer, P. Bäuerle, *Adv. Funct. Mater.* **2011**, *21*, 897–910; b) E. Lörtscher, *ChemPhysChem* **2011**, *12*, 2887–2889; c) E. J. Dell, B. Capozzi, K. H. DuBay, T. C. Berkelbach, J. R. Moreno, D. R. Reichman, L. Venkataraman, L. M. Campos, *J. Am. Chem. Soc.* **2013**, *135*, 11724–11727.

[12] a) H. Bürckstümmer, A. Weissenstein, D. Bialas, F. Würthner, *J. Org. Chem.* **2011**, *76*, 2426–2432; b) L. Huo, J. Hou, H.-Y.

Chen, S. Zhang, Y. Jiang, T. L. Chen, Y. Yang, *Macromolecules* **2009**, *42*, 6564–6571.

[13] E. M. Maya, P. Vázquez, T. Torres, *Chem. Eur. J.* **1999**, *5*, 2004–2013.

[14] A. Guerrero, S. Loser, G. Garcia-Belmonte, C. J. Bruns, J. Smith, H. Miyauchi, S. I. Stupp, J. Bisquert, T. J. Marks, *Phys. Chem. Chem. Phys.* **2013**, *15*, 16456–16462.